

Are Molecules Magical?

Non-Stabilizerness in Molecular Bonding

Matthieu Sarkis* and Alexandre Tkatchenko†

Department of Physics and Materials Science, University of Luxembourg, L-1511 Luxembourg City, Luxembourg

(Dated: April 10, 2025)

Isolated atoms as well as molecules at equilibrium are presumed to be simple from the point of view of quantum computational complexity. Here we show that the process of chemical bond formation is accompanied by a marked increase in the quantum complexity of the electronic ground state. By studying the hydrogen dimer H_2 as a prototypical example, we demonstrate that when two hydrogen atoms form a bond, a specific measure of quantum complexity exhibits a pronounced peak that closely follows the behavior of the binding energy. This measure of quantum complexity, known as *magic* in the quantum information literature, reflects how difficult it is to simulate the state using classical methods. This observation suggests that regions of strong bonding formation or breaking are also regions of enhanced intrinsic quantum complexity. This insight suggests a connection of quantum information measures to chemical reactivity and advocates the use of stretched molecules as a quantum computational resource.

Introduction—Quantum entanglement is a fundamental feature of many-body physics and quantum chemistry, reflecting nonclassical correlations between constituents [1–3]. It has become a key diagnostic in a wide range of systems—from condensed matter to molecular bonds—often quantified by measures such as the von Neumann entropy or Renyi entropies of reduced density matrices [4]. For example, in molecular systems such as the hydrogen molecule H_2 , entanglement between electrons is negligible when the atoms are far apart or nearly fused into a single nucleus, but grows as a covalent bond forms. However, it is now understood that entanglement alone is not a sufficient indicator of a quantum state’s computational complexity or *quantumness* [5, 6]. There exist highly entangled yet classically simulable states, notably the so-called *stabilizer states* that can be produced by Clifford gates—transformations belonging to the normalizer of the Pauli group—and efficiently simulated on a classical computer via the Gottesman-Knill theorem [7–9]. In other words, entanglement by itself does not guarantee quantum advantage. The resource that elevates a quantum state beyond stabilizer dynamics is referred to as *non-stabilizerness* or *magic*, as described by the resource theory of stabilizer quantum computation [5, 6, 10]. Stabilizer states and Clifford operations are considered *free* since they can be simulated efficiently on a classical computer, whereas non-stabilizer states provide the essential resource for transcending classical simulability. Magic can be quantified by various monotones that do not increase under stabilizer operations; one convenient measure is the *mana*, defined via the negativity of the state’s discrete Wigner function [6]. Indeed, stabilizer states possess a positive Wigner function, and for pure states, mana vanishes if and only if the state is a stabilizer state—a discrete analog of Hudson’s theorem linking positive Wigner representations to Gaussian states, thereby underlining that negativity in the quasiprobability distribution is essential for a state to supply quantum

computational advantage. Besides mana, other magic measures have been proposed, such as the *robustness of magic* [11–13] and the *stabilizer Renyi entropies* [14, 15]. Therefore, magic indicates the *quantum overhead* inherent in accurately modeling a system. If a molecular system has low magic, then a classical method might suffice. High magic, on the other hand, flags the need for quantum computational resources.

In parallel, quantum information concepts have begun to permeate the study of molecules and chemical bonding. The process of bond formation involves superposition of atomic configurations and entanglement between electrons. Measures such as entanglement entropy have been used to characterize these correlations in chemical systems. Rissler, Noack, and White [1] applied quantum information theory in chemistry by introducing orbital mutual information as a measure of electron interactions between orbitals, a concept that not only successfully identifies chemical bond patterns but also aids in optimizing DMRG algorithms. Building on this foundation, Boguslawski et al. [2] further developed the approach by calculating one- and two-electron entropies for molecular wavefunctions, thereby providing a more intuitive picture of electron correlation that informs the selection of active spaces. Recognizing the complexity of electron interactions, Ding et al. [16] refined these ideas by disentangling total orbital correlations into distinct classical and quantum components, which raised important questions regarding the genuine role of entanglement in chemical bonds. In a complementary effort, Szalay et al. [4] introduced a multiorbital correlation framework that utilizes genuine multipartite entanglement measures and clustering algorithms to reveal multi-center bonding patterns and to highlight the limitations of traditional bonding descriptions. Extending these insights to a more nuanced bonding analysis, Ding, Matito, and Schilling [3] proposed the concept of maximally entangled atomic orbitals (MEAOs), demonstrating that entanglement pat-

terms can capture both conventional two-center bonds and delocalized multicenter bonds, with the degree of multipartite entanglement serving as a quantitative index of bond strength and aromaticity. Finally, complementing these theoretical advances, Stein and Reiher [17] developed an automated protocol for active orbital space selection in multireference calculations, effectively leveraging entanglement measures to identify strongly correlated orbitals and streamline computational processes.

The goal of this work is to combine these quantum information non-stabilizerness insights with quantum chemistry. We conduct an analysis of the non-stabilizerness in the H_2 molecule as it forms and breaks a bond. By doing so, we aim to illustrate how concepts like magic, alongside more standard notions like entanglement together provide a more complete characterization of the electronic wavefunction's quantum nature. The rest of the paper is organized as follows. We first summarize the theoretical background and definitions of the various magic proxies used in this letter in the context of fermionic systems. We then describe our methodology for computing our reference *ab initio* ground state of the H_2 dimer across a range of interatomic distances. We finally present the results, showing the behavior of magic as a function of interatomic distance, and provides a discussion of our observations, and discuss in some possible experimental implications in the outlook section.

The Fermionic Wigner Function and Proxies of Magic—Non-stabilizerness concepts have been explored mostly in quantum spin chain context [18–24]. These notions can of course be defined for fermionic systems in various different ways. One possible trajectory is fermionization in the form of Jordan-Wigner transformation from a system of spin 1/2 degrees of freedom, following then the work of Wootters [25, 26]. Another direction could be to define a Grassmann valued phase space, and a notion of fermionic Wigner function defined thereof, following the seminal work of Cahill and Glauber [27]. We will instead follow the approach of [28–31] to leverage the structure of the Majorana group [32], fermionic analogue of the Pauli group, and define the fermionic Wigner function in terms of Majorana strings and discrete phase space.

Given a collection of n fermionic creation and annihilation operators c_p and c_p^\dagger , following [31, 32] we introduce for each mode the Hermitian Majorana operators $\eta_{2p-1} = c_p + c_p^\dagger$ and $\eta_{2p} = i(c_p - c_p^\dagger)$. We then define the Majorana strings

$$M_v = i^{v \cdot \Omega v} \eta_1^{v_1} \eta_2^{v_2} \dots \eta_{2n-1}^{v_{2n-1}} \eta_{2n}^{v_{2n}}, \quad (1)$$

where $v = (v_1, v_2, \dots, v_{2n-1}, v_{2n})^T \in (\mathbb{Z}_2)^{2n}$ is a binary vector, and Ω is a $(2n) \times (2n)$ square matrix with zeros on the diagonal, zeros on the upper-right triangle, and ones on the lower-left triangle. The prefactor $i^{v \cdot \Omega v}$ ensures Hermiticity of the Majorana strings. $\Gamma = (\mathbb{Z}_2)^{2n}$ plays here the role of discrete phase space for the fermionic system. The Majorana strings form a basis of Hermitian

operators, and given a quantum state represented by a density matrix ρ , one can decompose it in the Majorana basis as

$$\rho = \frac{1}{2^{2n}} \sum_{v \in \Gamma} \text{Tr}(\rho M_v) M_v. \quad (2)$$

We then call the quantity

$$W_\rho(v) = \text{Tr}(\rho M_v) \quad (3)$$

the fermionic Wigner function of the state ρ .

Given this fermionic Wigner function we define its L^p norm as

$$\|W_\rho\|_p = \left[\sum_{v \in \Gamma} |W_\rho(v)|^p \right]^{\frac{1}{p}}. \quad (4)$$

The α -stabilizer Renyi entropy is defined as

$$\mathcal{S}_\alpha = \frac{1}{1-\alpha} \log \left[\frac{\|W_\rho\|_{2\alpha}^{2\alpha}}{2^{2n}} \right]. \quad (5)$$

Following intuition from the discrete Wigner function of Wootters [25, 26], we define the mana as the L^1 norm instead:

$$\mathcal{M} = \log \left[\frac{\|W_\rho\|_1}{2^{2n}} \right]. \quad (6)$$

The filtered α -stabilizer Renyi entropy $\mathcal{F}\mathcal{S}_\alpha$ is defined like the α -stabilizer Renyi entropy but removes the often dominating contribution of the identity $v = (0, 0, \dots, 0)^T$ and parity operator $v = (1, 1, \dots, 1)^T$ from the sum defining the L^p norm [30], whose contribution can become dominant, especially in the large number of modes limit.

The L^p norms of the discrete Wigner function of a fermionic state capture how broadly the quantum state spreads over the discrete phase space Γ .

The H_2 dimer in second quantization: computing the ground state across dissociation—In the second quantization formalism, the electronic Hamiltonian (within the Born-Oppenheimer approximation) of a molecular system is expressed in terms of fermionic creation (c_p^\dagger) and annihilation (c_q) operators defined with respect to a chosen orbital basis. For a generic set of orbitals, the Hamiltonian is written as [33]

$$\hat{H} = \sum_{p,q} h_{pq} c_p^\dagger c_q + \frac{1}{2} \sum_{p,q,r,s} \langle pq|rs \rangle c_p^\dagger c_q^\dagger c_s c_r, \quad (7)$$

where h_{pq} are the one-body integrals (incorporating the kinetic energy of electrons and their interaction with the nuclei), $\langle pq|rs \rangle$ are the two-body integrals (accounting for electron-electron repulsion), and the quantum numbers p, q, r, s run over the complete set of orbitals in the basis [34, 35]. This non-relativistic field theory representation encapsulates all the many-body effects and provides

a convenient framework for *ab initio* quantum chemical calculations[36] [37, 38].

For the hydrogen dimer H_2 , we adopt the minimal STO-3G basis set, where each hydrogen atom is described by a linear combination of three Gaussian functions approximating the 1s atomic orbital. Despite its simplicity, the STO-3G basis offers a tractable, yet accurate model for exploring fundamental electronic properties of the hydrogen dimer.

To accurately determine the ground state of H_2 , we adopt an Unrestricted Hartree-Fock (UHF) approach, hence allowing different spatial orbitals for electrons of different spins (α and β), which is crucial for avoiding spin contamination [37, 38]. This is particularly important in the dissociation limit, where a restricted method would fail to describe the correct covalent bond breaking and yield unphysical results. Building upon the UHF solution, FCI is then employed to solve the electronic Schrödinger equation exactly within our STO-3G basis set [39]. FCI provides our benchmark for electron correlation, ensuring an accurate description of the ground state of the system across all interatomic distances.

Results and Discussion—The FCI ground state of the system is very well captured at any interatomic distance by a state of the form

$$|\psi(\theta)\rangle = \cos(\theta) |1100\rangle + \sin(\theta) |0011\rangle \quad (8)$$

with the ordering of the four fermionic modes given by: (i) spin α molecular orbital 0, (ii) spin β molecular orbital 0, (iii) spin α molecular orbital 1, and (iv) spin β molecular orbital 1. The second determinant corresponds to the fully excited state whose contribution is crucial for avoiding spin contamination in the large interatomic distance limit. The angle $\theta \equiv \theta(\ell)$ is a smooth function of the interatomic distance ℓ , connecting the large distance limit in which the system factorizes into a pair of independent hydrogen atoms to the interatomic distance regime of covalent bond formation. Indeed, at these large distances, the purely ionic contribution from the two determinants precisely cancel each other, leaving solely the purely covalent contribution. Around the bound state, the Hartree-Fock contribution alone provides instead a qualitatively good description of the ground state. The reader will find in Fig. 1 the binding energy curve of the H_2 molecule, namely the FCI energy

$$\mathcal{E}_{\text{FCI}}(\ell) = \langle \psi(\theta(\ell)) | \hat{H} | \psi(\theta(\ell)) \rangle \quad (9)$$

as a function of the interatomic distance, translated by the asymptotic contribution of two isolated hydrogen atoms $\mathcal{E}_{\text{FCI}}(\infty)$, as well as the angle θ defining the corresponding FCI ground state wavefunction.

Let us define the extrinsic curvature of the binding energy curve as

$$\kappa(\ell) = \frac{|\mathcal{E}_{\text{FCI}}''(\ell)|}{(1 + \mathcal{E}_{\text{FCI}}'(\ell)^2)^{3/2}}, \quad (10)$$

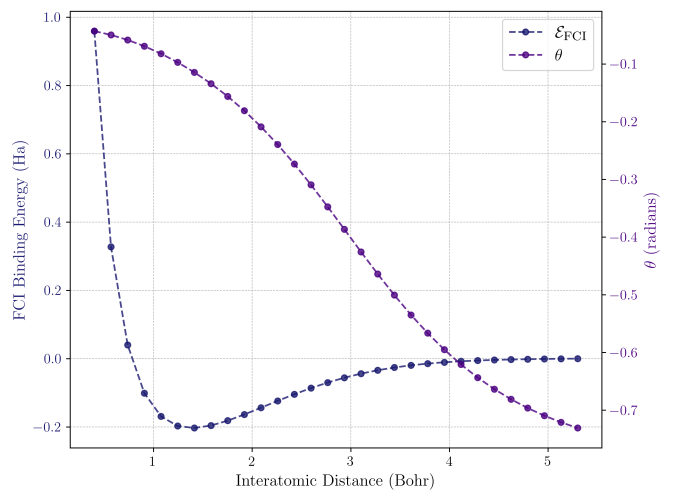


FIG. 1. FCI binding energy \mathcal{E}_{FCI} and θ angle defining the ground state wavefunction of the H_2 dimer as a function of the interatomic distance.

Let us denote by ℓ^* the point of maximal extrinsic curvature of the binding energy curve $\ell^* = \text{argmax}_{\ell} \kappa(\ell)$. For each value of the interatomic distance ℓ , we compute the fermionic Wigner function of the ground state and evaluate the magic proxies defined in the first Section of the paper. The reader will find in Fig. 2 the behavior of the stabilizer Renyi entropy \mathcal{S}_2 and the mana \mathcal{M} as a function of the interatomic distance ℓ .

Our results reveal a striking phenomenon: as the hydrogen atoms approach each other, the magic proxies develop a pronounced peak precisely at the interatomic distance where the extrinsic curvature of the binding energy curve is maximal. This suggests that the bonding process is accompanied by a significant increase in non-stabilizerness, implying that the formation of a covalent bond requires the consumption of a large amount of non-Clifford operations. As we discussed, a state with low magic is efficiently classically simulable, while high magic is a necessary ingredient for quantum computational speedup [6, 40]. Thus, our analysis indicates that the H_2 bond formation is not only a chemical process but also a transformation that incurs a cost in terms of quantum computational resources.

The angle θ defining the ground state wavefunction adjusts smoothly with ℓ , reflecting the relative weight of two determinants. In regions where the determinants contribute comparably, the interference between them amplifies off-diagonal correlations in the Majorana basis, leading to a more *spread out* fermionic Wigner function and, consequently, to a higher value of our magic proxies as defined by L^p norms of the fermionic Wigner function.

From the standpoint of molecular physics and quantum chemistry, our results offer an intriguing reinterpretation of chemical bond formation: in the dissociation

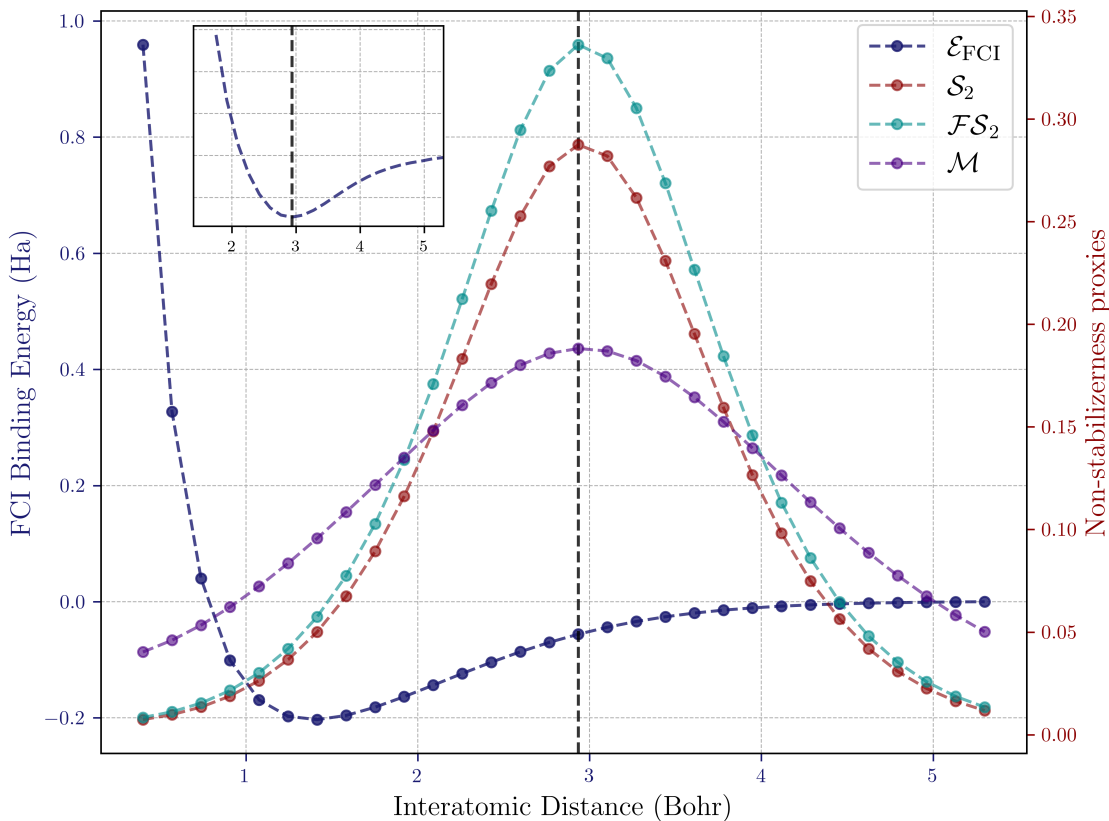


FIG. 2. Stabilizer Renyi entropy \mathcal{S}_2 , filtered stabilizer Renyi entropy \mathcal{FS}_2 , mana \mathcal{M} , and FCI binding energy \mathcal{E}_{FCI} as a function of the interatomic distance. These magic proxies exhibit a pronounced peak precisely at the value of the interatomic distance where the extrinsic curvature of the binding energy curve is extremized, as indicated by the vertical dashed line. The inset depicts the second derivative of the FCI binding energy, confirming the relation between the magic proxies and the curvature of the binding energy curve.

limit ($\ell \rightarrow \infty$), the hydrogen atoms are essentially isolated. The electronic wavefunction factorizes, leading to a state that is close to a product state. In such a regime, the fermionic correlations are minimal and the associated magic (or non-stabilizerness) is low, consistent with the notion of a classically tractable system.

At interatomic distances near ℓ^* , where the binding energy curve shows maximal extrinsic curvature, the wavefunction represents a delicate balance between the two determinants. This is the regime where the chemical bond is forming. The competition between the ionic and covalent contributions results in a highly correlated state. Our analysis shows that this is the very point at which the quantum state would demand a larger number of non-Clifford operations for its simulation, as reflected by the peak in magic proxies. The extrinsic curvature κ is a geometric measure of the sensitivity of the binding energy with respect to interatomic distance. Its maximum marks a rapid change in the energy landscape, signature of a transition in the electronic structure. This energetic reorganization is directly correlated with the rise in

non-stabilizerness, indicating that the very formation of the covalent bond is accompanied by an increase in the *quantumness* of the state.

Very interestingly, note that the ground state (8) can be understood as the state of a qubit upon interpreting the two determinants as computational basis states $|\tilde{0}\rangle = |1100\rangle$ and $|\tilde{1}\rangle = |0011\rangle$. We know that at very short interatomic distances, including the equilibrium bound state distance, the ground state of the system is very well approximated by setting $\theta \simeq 0$, namely by the state $|\tilde{0}\rangle$. Adiabatic increase of the bond length can then be interpreted as implementing the following unitary operation:

$$|\psi(\theta)\rangle = U(\theta) |\tilde{0}\rangle = \cos(\theta) |\tilde{0}\rangle + \sin(\theta) |\tilde{1}\rangle, \quad (11)$$

with $U(\theta)$ the rotation around the y -axis

$$U(\theta) = R_y(2\theta) = \begin{pmatrix} \cos \theta & -\sin \theta \\ \sin \theta & \cos \theta \end{pmatrix}. \quad (12)$$

Note that one can conjugate this rotation into a rotation

around the z -axis instead:

$$U(\theta) = R_x\left(\frac{\pi}{2}\right)R_z(2\theta)R_x\left(-\frac{\pi}{2}\right). \quad (13)$$

As explained below, the point of maximal magic corresponds to a value of the interatomic distance ℓ^* for which the angle θ is equal to $-\pi/8$. The key observation is the following: for $\theta = -\pi/8$, the unitary $U(-\pi/8)$ is precisely conjugate to the T-gate (more precisely to its Hermitian conjugate in our conventions), and *the conjugation matrix belongs to the Pauli group*. The T-gate is precisely known to be a non-Clifford gate which once adjoined to the group of Clifford operations allows for universal quantum computation. Moreover, conjugation by an element of the Pauli group does not impact non-stabilizerness, and therefore the adiabatic stretching of the bond from the equilibrium position of the dimer to the point of maximal extrinsic curvature of the FCI binding energy can indeed be interpreted as implementing a highly non Clifford gate. Conversely, the process of relaxing from the point of maximal extrinsic curvature towards the point of equilibrium of the dimer can be understood as implementing a T-gate. We push this reasoning further at the end of the outlook section.

The confluence of these perspectives reinforces a remarkable insight: the process of chemical bond formation is not solely an energetic or structural rearrangement but is also accompanied by a non-trivial transformation in the quantum informational character of the state. At large distances, the electrons are described by nearly independent, stabilizer-like states, whereas in the bonding formation region the superposition of covalent and ionic contributions requires an injection of magic into the system. This observation opens a conceptual bridge between quantum resource theories and chemical reactivity, suggesting that the cost of forming a bond can be viewed through the lens of quantum computational resources.

Remark concerning generalizability of the results to realistic basis sets, and analytical expression of the magic proxies—One can of course question whether the results observed above in the case of a minimal basis set generalize to richer, more expressive and realistic basis sets. Without entering into the technical details, let us show the results we obtain still in the case of the hydrogen dimer, but when employing the larger 6-31g basis set. The reader will find in Fig. 3 the depiction of the FCI binding energy curve and of the filtered 2-stabilizer Renyi entropy.

We still observe a neat pick in the magic proxy, but which appears slightly shifted to a larger interatomic distance with respect to the point of maximal extrinsic curvature of the binding energy curve. In the case of the hydrogen dimer, the use of a minimal basis set can already be considered relatively accurate, and as we saw leads to a perfect correlation between the point of maximal sensitivity, as characterized by the curvature data

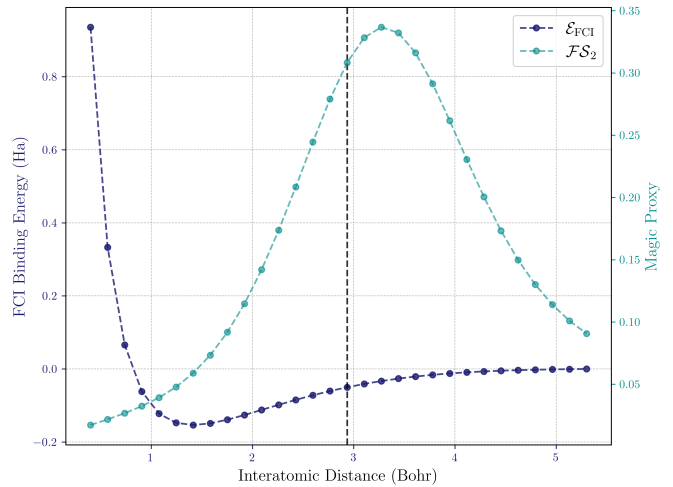


FIG. 3. FCI binding energy \mathcal{E}_{FCI} and filtered stabilizer Renyi entropy. One observes a slight shift to the right with respect to the point of maximal extrinsic curvature.

of the potential energy surface, and the maximality of non-stabilizerness. This points towards a deep connection between the non-classicality of molecular systems and the Riemannian geometry of their potential energy surface. We will comment more in the outlook section on the observed slight correction brought to this statement by the use of a larger basis set, i.e. by a more physically realistic setup.

Let us also mention that in the case of a minimal basis set for H_2 , the curse of dimensionality that plagues quantum chemistry for larger systems is absent, allowing for an analytic expression if the fermionic Wigner function, and therefore of the magic proxies. One can indeed easily see that among the 32 possible Majorana strings, 16 of them act diagonally in the space spanned by the two determinants, and 16 are off-diagonal and contribute to the cross term. Among the diagonal strings, depending on the relative contribution of the two determinants, 8 of them contribute $\cos^2(\theta) + \sin^2(\theta) = 1$ and 8 of them contribute $\cos^2(\theta) - \sin^2(\theta) = \cos(2\theta)$. Concerning the off-diagonal strings, 8 of them give a zero contribution, and the other 8 contribute $2 \sin(\theta) \cos(\theta) = \sin(2\theta)$. One can then extract the various magic proxies. For the stabilizer 2-Renyi entropy one obtains:

$$\mathcal{S}_2(\theta) = -\log \left[1 - \frac{\sin^2(4\theta)}{4} \right], \quad (14)$$

and for the mana:

$$\mathcal{M}(\theta) = \log \left[\frac{1 + |\cos(2\theta)| + |\sin(2\theta)|}{2} \right]. \quad (15)$$

We indeed check that at their common maximum $\theta(\ell^*) = -\pi/8$, these two quantities take respective values $\log(4/3) \simeq 0.227(6)$ and $\log\left(\frac{1}{2} + \frac{1}{\sqrt{2}}\right) \simeq 0.188(2)$,

as can be directly checked in Fig. 2. Though not scalable to more realistic basis sets and/or larger systems, one can therefore in principle prove the coincidence with the maximal extrinsic curvature point of the FCI binding curve.

Outlook—While our study focuses on the simple hydrogen dimer, it would be instructive to extend this analysis to more complex molecules. The methodology we employed – combining *ab initio* methods with quantum resource-theoretic measures – can be extended to other molecules and more sophisticated basis sets. One could, for instance, analyze the magic content in a stretched water molecule or in a transition metal dimer where multi-reference character is strong. We expect that systems requiring multi-reference descriptions will generally show non-zero mana.

Furthermore, it is worth emphasizing that the minimal STO-3G basis set, despite its simplicity, already reproduces the correct well-depth of H_2 with remarkable accuracy [37, 39]. This suggests that the essential physics of bond formation, the delicate balance between ionic and covalent contributions and the resulting rise in quantum correlations, is well captured even at this basic level of description. Consequently, we expect that the pronounced peak in magic proxies observed at the bond formation region is a robust feature that will persist when our approach is extended to heavier atoms and larger, more realistic basis sets. While such extensions may refine the quantitative details of both the binding energy curve and the magic measures, the qualitative behavior and specifically, the correlation between enhanced non-stabilizerness and the onset of covalent bonding, conceptually remain. One natural obstacle to scaling up to larger system lies in the exponential scaling of the number of Majorana string, i.e. of the fermionic phase space. However this could be handled through the evaluation of the magic proxies using Monte Carlo estimates [31].


The observed interplay between electronic structure and quantum computational resources suggests that quantum simulations of chemistry could benefit from incorporating magic measures as diagnostic tools. Understanding how magic is generated and consumed during chemical reactions could indeed inform the design of more efficient quantum algorithms for molecular modeling. For instance these insights may lead to the design of more efficient quantum algorithms that adapt to the changing resource demands along reaction coordinates.

Although magic is a computational resource concept, there may be indirect experimental signatures—such as changes in entanglement spectra or spectroscopic features—that correlate with the onset of high magic. Exploring these connections could provide a new experimental window into quantum correlations and non-stabilizerness in chemical systems. Our results indeed hint at a broader framework where concepts from quantum information theory beyond pure entanglement en-

tropy measures (like non-stabilizerness) can serve as indicators of physical phenomena like bonding in molecular systems. It would be enlightening to examine how mana scales with system size for a given chemical family, for example does adding more electrons in similar bonds increase the mana proportionally, or can mean-field capture most of it? Do peaks in magic proxies universally signal the formation of covalent bonds or reaction barriers? Investigating larger systems could therefore illuminate whether the degree of non-stabilizerness correlates with chemical reactivity or catalytic efficiency.

Finally, an intriguing perspective emerges when we consider harnessing the observed surge in non-stabilizerness as a resource for quantum computation. Imagine a protocol in which a dimer, initially at its equilibrium position, is adiabatically stretched, perhaps via coupling to an external field, to deliberately enhance the non-stabilizerness stored in its ground state. In this scenario, the dimer effectively serves as a reservoir of quantum magic that could later be coupled to an external device. Extending this idea to an array of dimers, one could control not only the spatial orientation and individual bond lengths but also the inter-dimer couplings, thereby engineering a system in which both non-stabilizerness and quantum correlations are actively leveraged for computational tasks. Interestingly, our observation that the peak in non-stabilizerness shifts slightly relative to the point of maximal extrinsic curvature when using a more realistic basis set is particularly promising. This shift implies that the system can be tuned to maximize magic without reaching the ‘risky’ regime where the covalent bond irreversibly breaks, ensuring that the dimer remains intact and reusable. Such a controlled extraction and subsequent utilization of non-stabilizerness could open up novel avenues for quantum simulation and computation.

Acknowledgments—M.S. would like to thank Junggi Yoon and Pablo Martinez Azcona for discussions, and Kyung Hee University for visits during the writing of this manuscript. The authors acknowledge funding via the FNR-CORE Grant “BroadApp” (FNR-CORE C20/MS/14769845) and ERC-AdG Grant “FITMOL”.

Code and Data Availability—The reader will find an open source python code to reproduce the results of this paper at .

* matthieu.sarkis@uni.lu
† alexandre.tkatchenko@uni.lu

- [1] J. Rissler, R. M. Noack, and S. R. White, *Chem. Phys.* **323**, 519 (2006).
- [2] K. Boguslawski and P. Tecmer, *Int. J. Quantum Chem.* **115**, 1289 (2015).

- [3] L. Ding, E. Matito, and C. Schilling, arXiv preprint arXiv:2501.15699 (2025).
- [4] S. Szalay, G. Barcza, T. Szilvási, L. Veis, and Ö. Legeza, *Sci. Rep.* **7**, 2237 (2017).
- [5] S. Bravyi and A. Kitaev, *Phys. Rev. A* **71**, 022316 (2005).
- [6] M. Howard, J. Wallman, V. Veitch, and J. Emerson, *Nature* **510**, 351 (2014).
- [7] D. Gottesman, *Stabilizer codes and quantum error correction. Caltech Ph. D.*, Ph.D. thesis, Caltech, eprint: quant-ph/9705052 (1997).
- [8] D. Gottesman, *Phys. Rev. A* **57**, 127 (1998).
- [9] S. Aaronson and D. Gottesman, *Phys. Rev. A* **70**, 052328 (2004).
- [10] S. Bravyi and J. Haah, *Phys. Rev. A* **86**, 052329 (2012).
- [11] M. Howard and E. Campbell, *Phys. Rev. Lett.* **118**, 090501 (2017).
- [12] M. Heinrich and D. Gross, *Quantum* **3**, 132 (2019).
- [13] H. Hamaguchi, K. Hamada, and N. Yoshioka, *Quantum* **8**, 1461 (2024).
- [14] L. Leone, S. F. Oliviero, and A. Hamma, *Phys. Rev. Lett.* **128**, 050402 (2022).
- [15] T. Haug and L. Piroli, *Quantum* **7**, 1092 (2023).
- [16] L. Ding, S. Mardazad, S. Das, S. Szalay, U. Schollwöck, Z. Zimborás, and C. Schilling, *J. Chem. Theory Comput.* **17**, 79 (2020).
- [17] C. J. Stein and M. Reiher, *J. Chem. Theory Comput.* **12**, 1760 (2016).
- [18] K. Goto, T. Nosaka, and M. Nozaki, arXiv preprint arXiv:2112.14593 (2021).
- [19] S. F. Oliviero, L. Leone, and A. Hamma, *Phys. Rev. A* **106**, 042426 (2022).
- [20] R. Smith, Z. Papic, and A. Hallam, arXiv preprint arXiv:2406.14348.
- [21] J. Odavić, M. Viscardi, and A. Hamma, arXiv preprint arXiv:2412.10228 (2024).
- [22] G. Passarelli, R. Fazio, and P. Lucignano, *Phys. Rev. A* **110**, 022436 (2024).
- [23] P. Tarabunga and C. Castelnovo, arXiv preprint arXiv:2311.08463.
- [24] P. S. Tarabunga, *Quantum* **8**, 1413 (2024).
- [25] W. K. Wootters, *Ann. Phys.* **176**, 1 (1987).
- [26] K. S. Gibbons, M. J. Hoffman, and W. K. Wootters, *Phys. Rev. A* **70**, 062101 (2004).
- [27] K. E. Cahill and R. J. Glauber, *Phys. Rev. A* **59**, 1538 (1999).
- [28] C. K. McLauchlan and B. Béri, *Phys. Rev. Lett.* **128**, 180504 (2022).
- [29] M. Mudassar, R. W. Chien, and D. Gottesman, *Phys. Rev. A* **110**, 032430 (2024).
- [30] M. Collura, J. De Nardis, V. Alba, and G. Lami, arXiv preprint arXiv:2412.05367 (2024).
- [31] S. Bera and M. Schirò, arXiv preprint arXiv:2502.01582.
- [32] V. Bettaque and B. Swingle, arXiv preprint arXiv:2407.11319 (2024).
- [33] The constant nuclear repulsion energy is omitted for simplicity, but of course contributes to the total energy of the system.
- [34] R. McWeeny, 2nd ed. (1989).
- [35] C. J. Cramer, *Essentials of computational chemistry: theories and models* (John Wiley & Sons, 2013).
- [36] For non-quantum chemists, we recommend the very nice paper [?] for a compact and self-contained exposition of some standards *ab initio* methods.
- [37] A. Szabo and N. S. Ostlund, *Modern quantum chemistry: introduction to advanced electronic structure theory* (Courier Corporation, 1996).
- [38] T. Helgaker, P. Jørgensen, and J. Olsen, *Molecular electronic-structure theory* (John Wiley & Sons, 2013).
- [39] W. J. Hehre, R. F. Stewart, and J. A. Pople, *J. Chem. Phys.* **51**, 2657 (1969).
- [40] V. Veitch, S. H. Mousavian, D. Gottesman, and J. Emerson, *New J. Phys.* **16**, 013009 (2014).